11,06,19

Thermophysical properties and barocaloric effect in ceramic ferroelectric NH_4HSeO_4

© V.S. Bondarev[1,2], E.A. Mikhaleva[1], E.V. Bogdanov[1,3], M.V. Gorev[1,2], M.S. Molokeev[1,2], I.N. Flerov[1,2]

[1] Kirensky Institute of Physics, Federal Research Center KSC SB, Russian Academy of Sciences, Krasnoyarsk, Russia
[2] Siberian Federal University, Institute of Engineering Physics and Radio Electronics, Krasnoyarsk, Russia
[3] Institute of Engineering Systems and Energy, Krasnoyarsk State Agrarian University, Krasnoyarsk, Russia

E-mail: vbondarev@yandex.ru

Received August 28, 2023
Revised August 28, 2023
Accepted September 1, 2023

The heat capacity, thermal expansion and hydrostatic pressure susceptibility of NH_4HSeO_4 ceramic samples have been investigated. The main parameters of the low temperature transitions between the para/pyroelectric (T_1) $\leftrightarrow$ incommensurate (T_2) $\leftrightarrow$ ferroelectric (T_3) $\leftrightarrow$ para/pyroelectric phases were determined. The phase $T-p$ diagram was refined and the baric coefficient dT_3/dp was determined. The volumetric strain behaviour and the results of direct measurements of $T_3(p)$ allowed us to establish the nature of the pressure effect on the stability of the ferroelectric phase. The extensive and intensive barocaloric effects were determined taking into account lattice thermal expansion.

Keywords: phase transitions, ferroelectrics, heat capacity, thermal expansion, pressure, barocaloric effect.

DOI: 10.61011/PSS.2023.10.57231.190

1. Introduction

Due to their rich sequence of crystalline phases and interesting individual physical properties, sulfates and selenates remain till now the subject of intense studies. Despite numerous publications relating to these crystals, there is still no sufficient information to fully describe their physical properties and unambiguously interpret the basic thermodynamic data.

Besides, ammonium sulfate, $NH_4NH_4SO_4$ (AS) [1–4], and its derivatives ammonium hydrogen sulfate, NH_4HSO_4 (AHS) [5–7], and ammonium hydroselenate, NH_4HSeO_4 (AHSe), are of interest as possible solid-state refrigerants with significant electrical, baric and piezocaloric effects, i.e. isothermal entropy changes (extensive effect, ΔS_{CE}) and adiabatic changes in temperature (intensive effect, ΔT_{AD}) when changing external electric field, hydrostatic or uniaxial pressure.

The crystal NH_4HSeO_4 is one of the most interesting representatives of these materials. In most experimental studies relating AHSe [8–11], phase transitions were registered at temperatures $T_3 \approx 100$ K, $T_2 \approx 250$ K and $T_1 \approx 260$ K. In the range of 100 to 250 K AHSe exhibits ferroelectric properties associated with the polarization existence along the axis *b*. In the temperature range 250–260 K between the ferroelectric and para/pyroelectric states there is a phase characterized in different papers as antiferroelectric [12] or incommensurate [13,14]. At the same time, AHSe is characterized by purely pyroelectric properties — polarization along the axis *c* exists in all phases, including in the paraelectric phase is much higher T_1. The characteristic feature of AHSe is the lack of consensus on the experimental phase diagrams $T(p)$, which differ in different papers not only in the magnitude, but also in the sign of the pressure coefficients dT/dp [15–16].

A number of papers documented the behavior features of the thermophysical properties of AHSe at other temperatures as well [17–18]. Detailed studies of AHSe depending of thermal history and mechanical treatment of the samples showed that the existing discrepancies can be attributed to the delicate equilibrium between metastable and stable phases [14,18].

In this paper comprehensive studies of the heat capacity, thermal expansion, and susceptibility to hydrostatic pressure of ceramic ammonium hydroselenate were carried out in a wide temperature range and near phase transitions in order to clarify the parameters of phase transitions and determine the ferroelectric phase resistance to hydrostatic pressure, and also barocaloric effects were studied.

2. Samples and experimental methods

Colorless single crystals of AHSe with volume 5–7 cm^3 were grown by isothermal evaporation of an aqueous solution at 305 K containing equimolar amounts of high-purity original substances $(NH_4)_2SeO_4$ and H_2SeO_4. All measurements were carried out on the same samples in the form of disks with diameter of 8 and thickness of 2 mm,

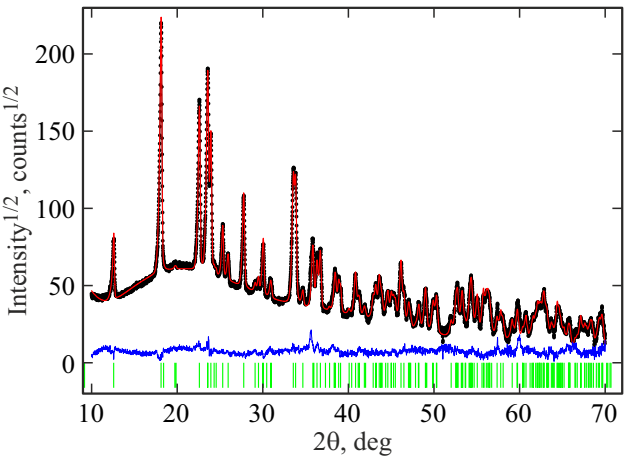

Figure 1. Results of NH_4HSeO_4 structure refinement by the Rietveld method.

prepared by pressing (~ 1 GPa) without heat treatment of crushed single crystals.

X-ray diffraction studies of AHSe samples were carried out at room temperature on a Haoyuan powder diffractometer with Cu-Kα radiation and a linear detector. The increment of detector 2θ was 0.01°, the exposure at each point was — 0.2 s per increment. The experimental diffraction pattern was used for analysis using the Rietveld method.

Firstly, monoclinic symmetry was discovered (sp. gr. $B112$, $Z = 6$), corresponding to the previously proposed [19,20], with lattice cell parameters in the studied samples $a = 19.7300(7)$ Å, $b = 4.60522(16)$ Å, $c = 7.5468(3)$ Å, $\beta = 102.606(2)$ deg, $V = 669.18(4)$ Å^3, and secondly, the absence of any additional phases was identified. Figure 1 shows the results of refinement by the Rietveld method ($R_{wp} = 10.487$, $R_p = 7.958$, $\chi^2 = 5.381$).

Studies of the temperature dependence of heat capacity $C_p(T)$ by the method of adiabatic calorimetry in the temperature range 78–280 K were carried out in continuous modes ($dT/dt = 0.15$–0.30 K/min) and discrete ($\Delta T = 0.05$–0.10 K) heating [21]. The measurements were performed on sample weighing 0.384 g. The heat capacity of the fittings was measured in the separate experiment. The error in the heat capacity determination did not exceed 0.3–0.5%.

Dilatometric studies were carried out on the sample used in calorimetric measurements. Experiments to determine the temperature behavior of linear deformation $\Delta L/L$ and the coefficient of linear thermal expansion α were performed on a DIL-402C induction dilatometer from NETZSCH in flow of dry helium gas (50 ml/min, volume concentration O_2 did not exceed 0.05%). The rod load on the sample was 30 cN. The sample heating rates in the temperature range 100–300 K varied from 2 to 4 K/min. A fused silica standard was used to calibrate and account for the expansion of the measurement system. The data obtained in several series of measurements agree with each other within 2–3%.

The hydrostatic pressure effect on the temperatures of heat capacity anomalies associated with phase transitions was experimentally studied by the DTA method. A sample with weight ~ 0.02 g was placed in a small copper container glued to one of the two junctions of Ge-Cu thermocouple. A quartz sample attached to another junction was used as a standard reference. The system mounted in this way was placed inside a high-pressure chamber of the cylinder-piston type, connected to a multiplier. Pressure up to 0.15 GPa was created using a mixture of pentane and silicon oil. Pressure and temperature were measured using a manganin pressure gauge and a copper-constantan thermocouple with an accuracy about $\pm 10^{-3}$ GPa and ± 0.3 K.

3. Results and discussion

Figure 2 shows molar heat capacity vs. temperature. A significant anomaly $C_p(T)$ with a maximum at temperature $T_3 = (106.2 \pm 0.5)$ K was identified, it corresponds to first order phase transition from low-temperature para/pyroelectric phase to ferroelectric one. Transitions from ferroelectric phase to the incommensurate phase (at $T_2 = 246.0 \pm 1.0$) and then to the high-temperature paro/pyroelectric phase (at $T_1 = 257.6 \pm 0.6$) are characterized by small, highly blurred heat capacity anomalies, which makes it difficult to accurately determine their temperatures.

To determine the integral characteristics of phase transitions, the heat capacity was divided into regular (lattice) $C_{Lat}(T)$ and anomalous $\Delta C_p(T)$ contributions associated with phase transitions. For this purpose, sections of the temperature dependence of the heat capacity outside the region of anomalies existence were considered as corresponding to $C_{Lat}(T)$ and were approximated by a combination of the Debye and Einstein functions

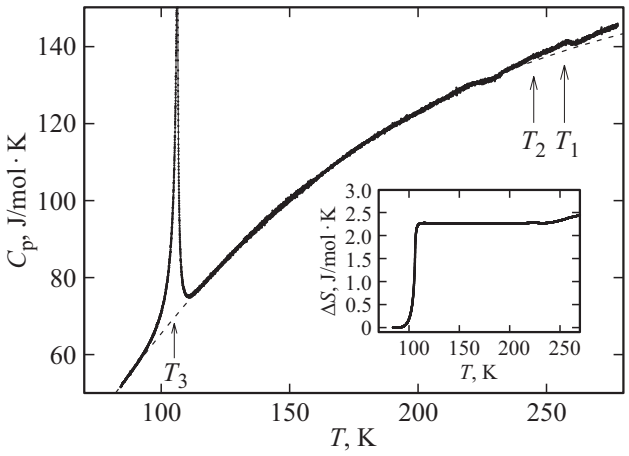

Figure 2. Temperature dependences of the molar heat capacity of ammonium hydroselenate and the anomalous entropy associated with the phase transition (in the insert). Dashed line — lattice heat capacity.

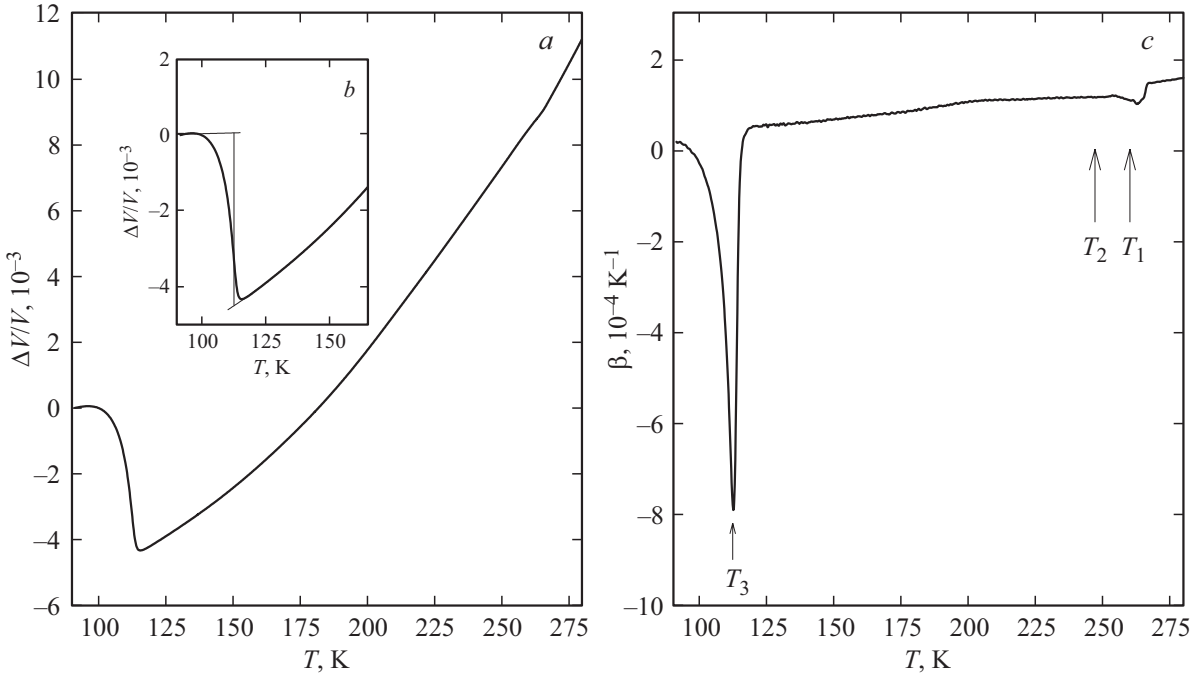

Figure 3. Temperature dependencies of volumetric deformation $\Delta V/V$ (a, b) and volumetric coefficient of thermal expansion β (c) NH_4HSeO_4.

$C_{\mathrm{Lat}}(T) = K_{\mathrm{D}}C_{\mathrm{D}}(T, \Theta_{\mathrm{D}}) + K_{\mathrm{E}}C_{\mathrm{E}}(T, \Theta_{\mathrm{E}})$, where K_{D}, K_{E}, Θ_{D}, Θ_{E} — adjustment parameters. Data below 235 K were used in the adjustment process. Above 235 K the experimental curve $C_{\mathrm{p}}(T)$ begins to deviate from $C_{\mathrm{Lat}}(T)$. This phenomenon may be associated with pre-transition effects of high-temperature transformation into the superionic phase [11].

By integrating the temperature dependence $\Delta C_{\mathrm{p}}/T$ the values and behavior of excess entropy are determined, see Figure 2. The entropy change during low-temperature phase transition is $\Delta S_3 = (2.3 \pm 0.1)$ J/mol · K, i. e. is significantly greater than the value $\Delta S_3 = 1.4$ J/mol · K previously determined for a powder sample by adiabatic calorimetry in discrete heating modes [22,23]. During high-temperature phase transitions the entropy change turned out to be very small ~ 0.05 J/mol · K, which is comparable to the value ~ 0.02 J/mol · K [22,23].

Figure 3 shows the temperature dependences of the volumetric characteristics of thermal expansion $\Delta V/V(T) = 3(\Delta L/L)(T)$ and $\beta(T) = 3\alpha$. Due to the significantly higher rate of temperature change in these experiments, the temperature T_3 of the low-temperature phase transition was found to be slightly higher (~ 110 K) than that determined in calorimetric measurements. Anomalies during transitions in the temperature range T_1 and T_2 are characterized by small, highly blurred anomalies $\beta(T)$, just like heat capacity anomalies.

The low-temperature transition is characterized by negative change in deformation $\Delta V_3/V = -(4.5 \pm 0.5) \cdot 10^{-3}$ and, therefore, in accordance with the Clapeyron-Clausius equation the negative pressure coefficient $\mathrm{d}T_3/\mathrm{d}p$.

The joint analysis of experimental calorimetric and dilatometric data made it possible to estimate the value of the pressure coefficient $\mathrm{d}T_3/\mathrm{d}p$ from the Clapeyron-Clausius equation $\mathrm{d}T/\mathrm{d}p = V_{\mathrm{m}}(\delta V/V)/\delta S$, where δV and δS — jumps in volume and entropy at the transition point. However, near the transition temperature, there is blurring of the anomalies of heat capacity and thermal expansion, due to both the imperfection of the samples, and the dynamic nature of the measurements of heat capacity and thermal expansion. Therefore, determination of the variables δV and δS at T_3 is very difficult and is associated with a large error. Approximate estimates based on the total entropy and volume changes during the phase transition give the value $\mathrm{d}T_3/\mathrm{d}p \approx -(120 \pm 20)$ K/GPa.

To determine $\mathrm{d}T_3/\mathrm{d}p$ we also used Pippard's relation [24], which establishes the relationship between the heat capacity and the coefficient of thermal expansion near the phase transition temperature, $C_{\mathrm{p}} = V_{\mathrm{m}}T_3\beta/(\mathrm{d}T_3/\mathrm{d}p) + \mathrm{const}$. Figure 4 demonstrates that this relationship is quite well met in the temperature range 97−103.5 K and gives the value $\mathrm{d}T_3/\mathrm{d}p \approx -(100 \pm 20)$ K/GPa.

Experimental phase $T-p$-diagram and temperature dependences of DTA signal at different pressures in region of low-temperature phase transition are given in Figure 5. At very low pressure a decrease in DTA signal was observed compared to the anomaly at $p = 0$, but further increase in pressure practically had no effect on this parameter (Figure 5, b). Most likely, this phenomenon is associated with the increase under pressure of the thermal conductivity of the medium in which the test sample is located.

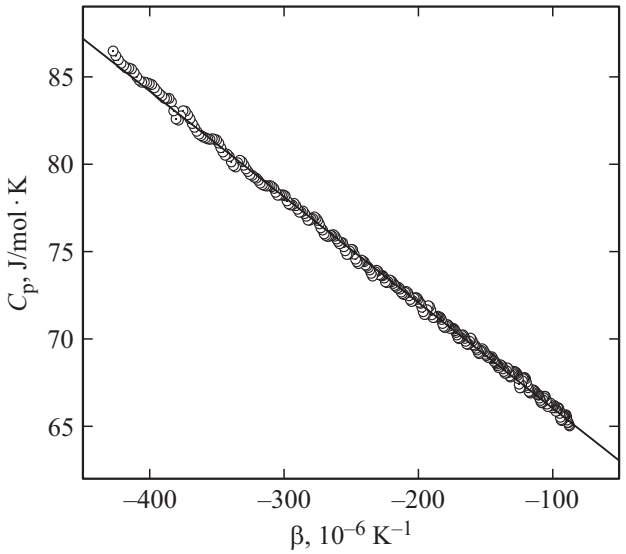

Figure 4. Molar heat capacity C_p vs. coefficient of volumetric thermal expansion β below T_3.

A small DTA anomaly does not allow us to make an unambiguous conclusion about the dependence on pressure of the entalphy, and entropy jump during first order phase transition. Under pressure DTA anomalies shift to the region of low temperatures (Figure 5, *a*). The corresponding pressure coefficient was $dT_3/dp = -(74 \pm 2)$ K/GPa.

The difference in the values of dT_3/dp, determined experimentally and calculated by different methods, can be explained by different degrees of blurring of the dependencies $C_p(T)$ and $\beta(T)$ due to experiments on ceramic samples with different rates of temperature change in the processes of measuring heat capacity and thermal expansion, as well as the possible texture of the sample. Nevertheless, the agreement between the experimental and calculated pressure coefficients can be considered quite satisfactory. As noted above, literature data on the parameters of phase transitions in ammonium hydroselenate are very contradictory. In particular, the pressure coefficients dT_3/dp, determined by different methods, differ even in sign: 200 K/GPa [15]; and -52 K/GPa [16]. The last value dT_3/dp, determined by measuring the dielectric properties under pressure, is close to the value we obtained through direct studies of the pressure effect on the thermal properties of AHSe, which are neutral with respect to nature of phase transformations. Indirect evidence of the offset T_3 towards low temperatures is the determined by us negative sign of the deformation change. Thus, considering that by absolute value of dT_3/dp is greater than $dT_2/dp = -21$ K/GPa [16], the hydrostatic pressure leads to expansion of the temperature region of spontaneous polarization existence.

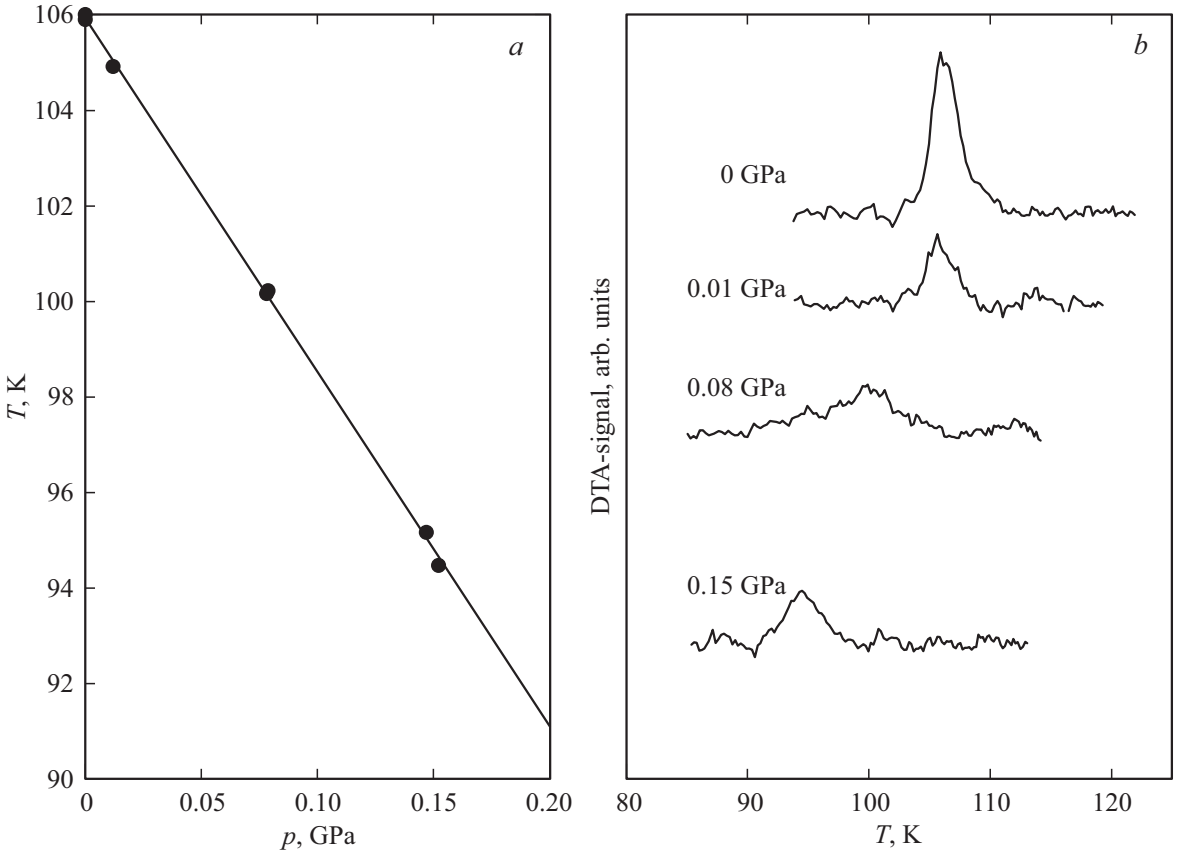

Figure 5. Phase $T-p$-diagram (*a*) and temperature dependences of DTA signal at different pressures (*b*) in the region of low-temperature phase transition.

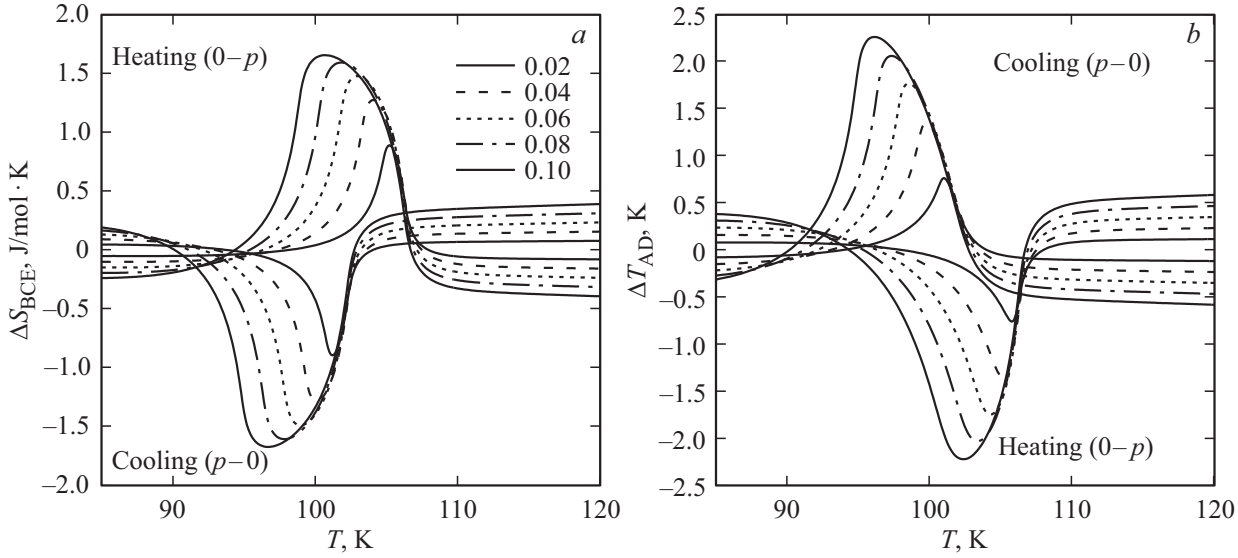

Figure 6. Temperature dependences of the extensive, ΔS_{BCE}, and intensive, ΔT_{AD}, BCE, taking into account the change in lattice entropy when pressure is applied and removed.

4. Barocaloric effect

The data obtained allowed us to analyze extensive and intensive barocaloric effects (BCE) within the framework of the method we proposed earlier and used in the study of a number of families of crystals [3,5–7,25,26]. Taking into account very small entropy and deformation changes during phase transitions from the ferroelectric phase to the incommensurate and then paraelectric phases in the region 220−260 K only caloric effects in the transition region at T_3 were analyzed in detail.

Information on the dependences of barocaloric entropy (extensive BCE), ΔS_{BCE}, on temperature and pressure was obtained by analyzing the total entropy of AHSe at $p = 0$ and $p \neq 0$ under isothermal conditions

$$\Delta S_{\mathrm{BCE}}(T, p) = S(T, p) - S(T, 0), \tag{1}$$

and the adiabatic change in temperature (intensive BCE) with change in pressure, ΔT_{AD}, was determined from the relation

$$S(T + \Delta T_{\mathrm{AD}}, p) = S(T, 0). \tag{2}$$

For $p = 0$ the total entropy of the compounds, $S(T, 0)$, as well as the anomalous, $\Delta S(T, 0)$, and lattice, $S_{\mathrm{Lat}}(T, 0)$, contributions were determined by analyzing heat capacity data $C_{\mathrm{p}}(T, 0)$

$$S(T, 0) = S_{\mathrm{Lat}}(T, 0) + \Delta S(T, 0). \tag{3}$$

The hydrostatic pressure influence on the behavior of total entropy was not established experimentally, therefore its temperature dependences at various pressures are calculated by summing the lattice entropy and the entropy of anomalous contributions

$$S(T, p) = S_{\mathrm{Lat}}(T, 0) + \Delta S_{\mathrm{Lat}}(T, p) + \Delta S(T, p). \tag{4}$$

It was assumed that the entropy of the phase transition, ΔS_3, as well as the degree of its proximity to the tricritical point do not depend on pressure. The position of the anomalous entropy at different pressures $\Delta S_3(T, p)$ was determined by the shift of the function $\Delta S_3(T, 0)$ at $p = 0$ along the temperature scale in accordance with the pressure coefficient $\mathrm{d}T_3/\mathrm{d}p$

$$\Delta S_3(T, p) = \Delta S_3(T + p \cdot \mathrm{d}T_3/\mathrm{d}p, 0). \tag{5}$$

The change in the volume of the crystal lattice under pressure leads to change in the total entropy of solids and in some cases can play significant role in the formation of the barocaloric effect. This follows from Maxwell's equation $(\partial S_{\mathrm{Lat}}/\partial p)_{\mathrm{T}} = -(\partial V_{\mathrm{Lat}}/\partial T)_{\mathrm{p}}$, which shows that the change in isothermal entropy is proportional to the volumetric coefficient of thermal expansion β_{Lat},

$$\Delta S_{\mathrm{Lat}}(T, p) = -\int \left[\partial V_{\mathrm{Lat}}/\partial T\right] \cdot \mathrm{d}p \approx -V_{\mathrm{m}} \cdot \beta_{\mathrm{Lat}}(T) \cdot p. \tag{6}$$

Here it is assumed that the molar volume V_{m} and the coefficient β_{Lat} depend weakly on pressure.

Transformations of the first order are accompanied by hysteresis of temperature and pressure, δT and δp, which shall be taken into account in order to avoid errors in determining actual BCEs due to the effect of irreversibility of the heating/cooling and application/removal of pressure processes.

For phase transitions characterized by a negative pressure coefficient, $\mathrm{d}T/\mathrm{d}p < 0$, barocaloric effects upon application $(0 \to p)$ and removal $(p \to 0)$ of pressure are determined using data on the temperature dependences of entropy in

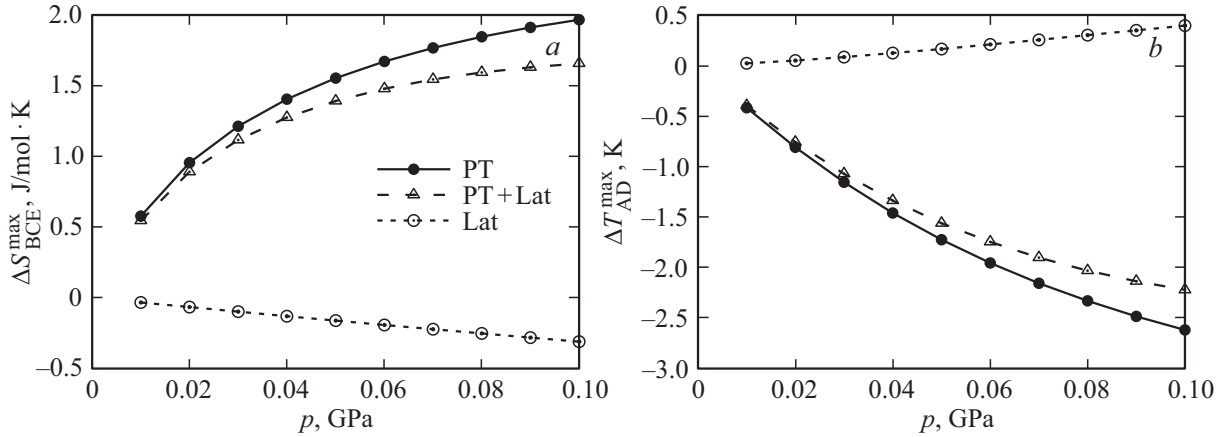

Figure 7. Pressure dependences of maximum values of extensive (a) and intensive (b) BCEs, obtained without consideration (PT) and with consideration (PT + Lat) of thermal expansion of the crystal lattice, as well as lattice contributions (Lat).

heating modes, S_H, and cooling modes, S_C,:

$$\Delta S_{BCE}(T, p \to 0) = S_C(T, 0) - S_C(T, p),$$
$$\Delta S_{BCE}(T, 0 \to p) = S_H(T, p) - S_H(T, 0),$$
$$\Delta T_{AD}(T, p \to 0) = T(S_C, 0) - T(S_C, p),$$
$$\Delta T_{AD}(T, 0 \to p) = T(S_H, p) - T(S_H, 0). \qquad (7)$$

The dependences of extensive, ΔS_{BCE}, and intensive, ΔT_{AD}, effects on temperature at different pressures calculated using relations (7) are shown in Figure 6.

Due to the presence of hysteresis $\delta T_3 \approx 4.5\,\mathrm{K}$ [22] the reversible extensive BCE is observed at pressures $p_{rev} \geq \delta T_3/(\mathrm{d}T_3/\mathrm{d}p) \approx 0.05\,\mathrm{GPa}$.

Figure 7 shows the pressure dependences of the maximum values ΔS_{BCE} and ΔT_{AD}, as well as individual contributions associated with both phase transition ($\Delta S_{BCE}^{PT} > 0$ and $\Delta T_{AD}^{PT} < 0$), and with change in lattice entropy ($\Delta S_{BCE}^{Lat} < 0$ and $\Delta T_{AD}^{Lat} > 0$). The variable ΔS_{BCE}^{PT} with pressure increasing tends to its maximum possible value, equal to ΔS_3.

The opposite signs of the anomalous and lattice BCE lead to a decrease in the total effects ΔS_{BCE} and ΔT_{AD}. Maximum possible extensive BCE $\Delta S_{BCE}^{max} \approx 1.7\,\mathrm{J/mol \cdot K} = 10.5\,\mathrm{J/kg \cdot K}$ in the studied ammonium hydroselenate can be achieved at pressure $\sim 0.1\,\mathrm{GPa}$, and the maximum intensive BCE, $\Delta T_{AD}^{max} \approx -2.5\,\mathrm{K}$, is realized at a higher pressure $\sim 0.15-0.20\,\mathrm{GPa}$.

Barocaloric effects in ammonium hydroselenate turned out to be not so significant compared to similar parameters of our previously studied AHS [5–7], considered as a promising working working body in solid-state refrigerators with high cooling capacity. In our opinion, this may be due to change in chemical pressure caused by the replacement of the central atom, Se → S, which led to significant ordering of the structure at room temperature and, as a consequence, to small entropy changes at low temperature phase transitions.

5. Conclusion

The study of the heat capacity, thermal expansion and susceptibility to hydrostatic pressure of ammonium hydroselenate, NH_4HSeO_4, identified the following.

Below room temperature, property anomalies associated with phase transitions between para/pyroelectric (T_1) ↔ incommensurate (T_2) ↔ ferroelectric (T_3) ↔ para/pyroelectric phases) were detected. As a result of thermal cycling the experiments involving measurements of heat capacity and thermal expansion did not identify significant changes in temperatures and the sequence of phase transitions, as well as the formation of metastable phases.

Detailed calorimetric studies made it possible to reliably establish changes in entropy during phase transitions and the temperature ranges of their existence. Three independent methods were used to determine the susceptibility to hydrostatic pressure of temperature of transition between the ferroelectric and low-temperature para/pyroelectric phases. The expansion of the temperature range of stability of the ferroelectric phase under pressure is confirmed by the negative signs of the pressure coefficient $\mathrm{d}T_3/\mathrm{d}p$ and changes in spontaneous deformation.

Extensive and intensive barocaloric effects were determined, they turned out to be not so significant in comparison with the parameters of materials that are promising for use as working working bodies in solid-state refrigerators with high cooling capacity. However, due to the very low hydrostatic pressure ($< 0.1\,\mathrm{GPa}$) required to achieve maximum barocaloric parameters of AHSe, it can be considered as a rather adequate solid refrigerant in the refrigeration cycles of small-sized cooling devices.

Acknowledgments

X-ray and and dilatometric data were obtained using the equipment of the Krasnoyarsk Regional Center for Collective Use of the Federal Research Center, Krasnoyarsk Scientific Center of the Siberian Branch of the Russian Academy of Sciences.

Funding

The study was supported by the grant of the Russian Science Foundation No. 23-22-10014, Krasnoyarsk Regional Science Foundation, https://rscf.ru/en/project/23-22-10014/.

Conflict of interest

The authors declare that they have no conflict of interest.

References

[1] P. Lloveras, E. Stern-Taulats, M. Barrio, J.-L. Tamarit, S. Crossley, W. Li, V. Pom-jakushin, A. Planes, L. Mañosa, N.D. Mathur, X. Moya. Nature Commun. **6**, 8801 (2015).
[2] V.S. Bondarev, E.A. Mikhaleva, M.V. Gorev, I.N. Flerov. J. Alloys Compd. **892**, 162130 (2022).
[3] E. Mikhaleva, M. Gorev, V. Bondarev, E. Bogdanov, I. Flerov. Scripta Materialia 191, **149** (2021).
[4] S. Crossley, W. Li, X. Moya, N.D. Mathur. Philos. Trans. A Math. Phys. Eng. Sci. **374**, 20150313 (2016).
[5] E.A. Mikhaleva, I.N. Flerov, A.V. Kartashev, M.V. Gorev, E.V. Bogdanov, V.S. Bondarev. Solid State Sci. **67**, 1 (2017).
[6] E.A. Mikhaleva, I.N. Flerov, V.S. Bondarev, M.V. Gorev, A.D. Vasiliev, T.N. Davydova. Ferroelectrics **430**, *1*, 78 (2012).
[7] E.A. Mikhaleva, M.V. Gorev, M.S. Molokeev, A.V. Kartashev, I.N. Flerov. J. Alloys Compd. **839**, 155085(2020).
[8] R. Poprawski, J. Dziedzic. J. Phys. Chem. Solids **45**, 355 (1984).
[9] Ph. Colomban, A. Rozycki. A. Novak. Sollid State Commun. **67**, 969 (1988).
[10] J. Przeslawski, B. Kosturek, Z. Chapla. Ferroelectrics **401**, 79 (2010).
[11] R. Poprawski. Solid State Commun. **67**, 629 (1988).
[12] Z. Czafla. Acta Univ. Wratislaviensis **550**, 1 (1985).
[13] I.P. Aleksandrova, O.V. Rosanov, Yu.A. Sukhovsky, Yu.A. Moskvich. Phys. Lett. A **95**, 339 (1983).
[14] I.P. Aleksandrova, Ph. Colomban, F. Denover, N.Le. Calve, A. Novak, B. Pasquier, A. Rozycki. Phys. Status Solidi A **111**, 531 (1989).
[15] V.S. Krasikov, L.I. Zherebtsova, M.P. Zaitseva. FTT **23**, 289 (1981). (in Russian).
[16] R. Poprawski. Ferroelectrics **124**, 415 (1991).
[17] R. Poprawski, I. Dziedzic, W. Bronowska. Acta Phys. Pol. A **63**, 601 (1983).
[18] Ph. Colomban, A. Rozycki, A. Novak. Solid State Commun. **67**, 969 (1988).
[19] I.P. Makarova, L.A. Muradyan, E.E. Rider, V.A. Sarin, I.P. Alexandrova, V.I. Simonov. Kristallografiya **35**, 647 (1990). (in Russian).
[20] I.P. Makarova. Acta Crystallogr. B **49**, 11 (1993).
[21] A.V. Kartashev, I.N. Flerov, N.V. Volkov, K.A. Sablina. FTT **50**, *11*, 2027 (2008). (in Russian).
[22] R. Popravski, P.S. Smirnov, B.A. Strukov. FTT **25**, 1339 (1984). (in Russian).
[23] R. Poprawski, S.A. Taraskin. Ferroelectrics **79**, *1*, 245 (1988).
[24] A.B. Pippard. The Elements of Classical Thermodynamics. Cambridge University Press, N.Y. (1964).
[25] M. Gorev, E. Bogdanov, I. Flerov. J. Phys. D **50**, *38*, 384002 (2017).
[26] M.V. Gorev, E.V. Bogdanov, I.N. Flerov. Scr. Mater. **139**, 53 (2017).

Translated by I.Mazurov